Thermal annealing effects on ultra-violet luminescence properties of Gd doped AlN

Kita, Takashi ; Ishizu, Yuta ; Tsuji, Kazuma ; Harada, Yukihiro ; Chigi, Yoshitaka ; Nishimoto, Tetsuro ; Tanaka, Hiroyuki ; Kobayashi,…

(Citation)
Journal of Applied Physics,117(16):163105-163105

(Issue Date)
2015-04-28

(Resource Type)
journal article

(Version)
Version of Record

Thermal annealing effects on ultra-violet luminescence properties of Gd doped AlN

Takashi Kita, Yuta Ishizu, Kazuma Tsuji, Yukihiro Harada, Yoshitaka Chigi, Tetsuro Nishimoto, Hiroyuki Tanaka, Mikihiro Kobayashi, Tsuguo Ishihara, and Hirokazu Izumi

Citation: Journal of Applied Physics **117**, 163105 (2015); doi: 10.1063/1.4919419
View online: http://dx.doi.org/10.1063/1.4919419
View Table of Contents: http://scitation.aip.org/content/aip/journal/jap/117/16?ver=pdfcov
Published by the AIP Publishing

JOURNAL OF APPLIED PHYSICS **117**, 163105 (2015)

Thermal annealing effects on ultra-violet luminescence properties of Gd doped AlN

Takashi Kita,[1] Yuta Ishizu,[1] Kazuma Tsuji,[1] Yukihiro Harada,[1] Yoshitaka Chigi,[2] Tetsuro Nishimoto,[2] Hiroyuki Tanaka,[2] Mikihiro Kobayashi,[2] Tsuguo Ishihara,[3] and Hirokazu Izumi[3]

[1]*Department of Electrical and Electronic Engineering, Graduate School of Engineering, Kobe University, 1-1 Rokkodai, Nada, Kobe 657-8501, Japan*
[2]*YUMEX INC., 400 Itoda, Yumesaki, Himeji, Hyogo 671-2114, Japan*
[3]*Hyogo Prefectural Institute of Technology, 3-1-12 Yukihira, Suma, Kobe 654-0037, Japan*

(Received 13 February 2015; accepted 20 April 2015; published online 29 April 2015)

We studied energy transfer from AlN to doped Gd^{3+} ions as a function of the post-thermal annealing temperature. Gd-doped AlN thin films were deposited on fused-silica substrates using a reactive radio-frequency magnetron sputtering technique. The film is a *c*-axis oriented polycrystal. The intra-orbital electron transition in Gd^{3+} showed an atomically sharp luminescence at 3.9 eV (318 nm). The photoluminescence (PL) excitation spectrum exhibited a resonant peak, indicating efficient energy transfer from the host AlN crystal to Gd^{3+} ions. The PL intensity increases approximately ten times by thermal annealing. The PL decay lifetime becomes long with annealing, and mid-gap luminescence relating to the crystal defects in AlN was also found to be reduced by annealing. These results suggest that energy dissipation of excited carriers in AlN was suppressed by annealing, and the efficiency of energy transfer into Gd^{3+} was improved. © *2015 AIP Publishing LLC*.
[http://dx.doi.org/10.1063/1.4919419]

I. INTRODUCTION

Ultraviolet (UV) light sources have been used in a diverse variety of applications such as photolithography, photo-polymerization, sterilization, medical treatments for incurable skin diseases,[1] and the efficient generation of vitamins D_2 and D_3.[2] Ever since the invention of the mercury lamp in 1927, its bright UV light has been widely used. However, the lamps include harmful constituents and have serious issues, such as short bulb lifetime and low emission efficiency. Similar problems affect excimer lamps. Recently, UV light-emitting diodes (LEDs) have been extensively explored because of their attractive properties such as high emission efficiency and good wavelength controllability.[3–6] The LED emission wavelengths cover the UVA, UVB, and UVC wavelength regions. However, UV LEDs are point light sources, and their spectral line width is generally broad as a result of band-to-band emission; these features are undesirable for several key applications such as photolithography and medical treatments. These demand a large-scale UV-light panel with an atomically sharp luminescence line. The spatial resolution of photolithography improves with decreasing linewidth of the light source, and a uniformly emitting large area light panel instead of using a point light source of UV-LEDs is useful. On the other hand, the application of the narrow band UV-light source is indispensable for medical treatments, because a narrow band less than a few nm can avoid serious risks causing skin cancer and simultaneously earns the best photo-therapy effect.

We propose a novel light source for the practical realization of spectrally sharp UV-light emitting devices using atomic transitions in rare-earth phosphors. The intra-4*f* electron transition in rare-earth ions is atomically sharp, and the temperature drift of the emission wavelength is negligible because of the occupied outer orbitals. As a host material for rare-earth elements with emission over a wide wavelength range, wide-band gap nitride semiconductors such as AlN, GaN, and $Al_xGa_{1-x}N$ have been explored[7–26] for developing electroluminescence devices[10,22–24] and electron-excitation devices.[25,26] In particular, for UV rare-earth phosphors, lightly Gd-doped AlN or $Al_xGa_{1-x}N$ is known to emit an atomically sharp line at approximately 3.9 eV (318 nm).[13–21,24–26] We have reported the emission properties of lightly Gd-doped AlN ($Al_{1-x}Gd_xN$) polycrystalline thin films fabricated by using a reactive sputtering technique[19–21,25,26] and developed a bright UV emitter pumped by an electron beam.[25,26] The maximum output power we achieved was greater than 1.0 mW/cm^2.[26] The intense UV emission is realized by efficient indirect excitation in which the energy absorbed in AlN is transferred to the higher excited states of Gd^{3+}, which then relax to the lowest excited state $^6P_{7/2}$ and generates the sharp luminescence by the transition to the ground state $^8S_{7/2}$.[13–21] In contrast to direct excitation of lightly doped rare-earth ions, indirect excitation is rather efficient because the host semiconductor acts as an effective energy absorber with a large optical-excitation cross section. Recently, we found several resonant energy-transfer channels for indirect excitation in thermally annealed Gd-doped AlN films.[21] Post-thermal annealing has drastically improved the UV luminescence efficiency. In this work, we systematically studied thermal annealing effects on the atomically sharp UV luminescence at 3.9 eV (318 nm) of Gd^{3+} ions doped in AlN. Thermal annealing dramatically enhances the luminescence intensity.

We discuss a key influencing on the efficiency of the energy-transfer from AlN to Gd^{3+}.

II. GROWTH OF $Al_{1-x}Gd_xN$ THIN FILMS AND CHARACTERIZATION TECHNIQUES

$Al_{1-x}Gd_xN$ thin films were grown on fused-silica substrates using a reactive radio-frequency (RF) magnetron sputtering technique. A growth chamber equipped with three targets is separated from a substrate-introduction chamber. The back pressure of the growth chamber was 1.0×10^{-6} Pa, a value identical to that used for molecular-beam epitaxy. We used an ultrapure (99.9999%) gas mixture of argon and nitrogen for the reactive growth, and the partial pressure ratio was even. The argon and nitrogen flow rates were precisely controlled using a flow rate controller and adjusted to keep the total sputtering pressure at 5.0 Pa. An Al (99.99%) disk was used as a target for AlN growth. When growing $Al_{1-x}Gd_xN$, we set Gd (99.9%) metal tips on an Al target. The GdN mole fraction x was controlled by changing the number of Gd tips on the Al target. The mole fraction x estimated by the electron probe microanalyzer was 0.003. All thin films were grown at 200 °C, and the input RF power was 250 W during the growth. The growth rate of AlN and $Al_{0.997}Gd_{0.003}N$ was 7 nm/min. First, we grew a 700-nm-thick AlN buffer layer on a fused-silica substrate. Subsequently, a 700-nm-thick $Al_{0.997}Gd_{0.003}N$ film was deposited on it. Secondary-ion mass-spectroscopic (SIMS) analysis on the as-deposited $Al_{0.997}Gd_{0.003}N$/AlN film showed that the oxygen content was approximately 1.0×10^{19} cm^{-3}. Besides, the characteristic parameters of S (shape) and W (wing) obtained from the positron annihilation spectroscopy[27] for the as-deposited film were 0.49 and 0.0135, respectively. The S and W parameters represent a change in the energy distribution of the annihilation γ ray due to positron-electron pairs with a low-momentum distribution and a change due to pairs with a high-momentum distribution, respectively. Vacancy-type defects increase S and decrease W. The evaluated S and W parameters of our as-deposited film are comparable to epitaxial films grown by NH_3-source molecular beam epitaxy.[27] We carried out post-thermal annealing for 30 min at 500, 700, and 900 °C under a continuous flow of highly purified N_2. The ramp-up time up to the annealing temperature from room temperature was 30 s.

We analyzed the crystal orientation and the lattice constant using X-ray diffraction (XRD) of the Cu-K_α line ($\lambda = 0.15418$ nm). The out-of-plane XRD spectrum of the as-deposited film shows a strong peak at the (0002) plane, indicating a c-axis preferential orientation.[16] Conversely, an in-plane XRD spectrum shows various diffraction lines arising from different crystal planes, and the X-ray pole figure of the in-plane component shows a clear ring pattern. This indicates that the deposited $Al_{0.997}Gd_{0.003}N$/AlN thin film is a c-axis-oriented polycrystal. The tilting angle of the c-axis was within 6°, according to the X-ray rocking curve. The X-ray diffraction properties were almost independent of post-thermal annealing except for a slight increase in the (0002)-diffraction intensity with the annealing temperature.

The photoluminescence (PL) spectrum, PL excitation (PLE) profile, and time-resolved PL spectrum were measured by a spectrophotometer (Hitachi High Technologies F7000) equipped with a Xe lamp as the excitation source. The PL was spectrally dispersed by a monochromator and detected using a photomultiplier tube. The spectral resolution of this monochromatic system was approximately 1.5 meV at 3.9 eV (318 nm). Light pulses were generated by mechanically chopping the Xe lamp. The pulse duration was 1.5 ms, and the repetition rate was 40 Hz. The temporal resolution of our detection system was 10 μs. The sample was mounted in a closed-cycle cryostat that can control the temperature in the range of 13–300 K.

III. THERMAL ANNEALING EFFECTS ON ATOMICALLY SHARP UV LUMINESCENCE AND ITS EXCITATION STRUCTURE

Figure 1(a) shows typical PL results of the as-deposited $Al_{0.997}Gd_{0.003}N$/AlN thin film measured at 300 K. The excitation energy was 6.20 eV (200 nm), which is close to the fundamental band edge of bulk AlN.[28,29] We observed a sharp luminescence line at ~3.9 eV (318 nm). The inset displays the high resolution PL spectrum. The fine PL structure corresponds to the transition from the lowest excited state $^6P_{7/2}$ to the ground state $^8S_{7/2}$.[13–21] Gruber *et al*. reported that

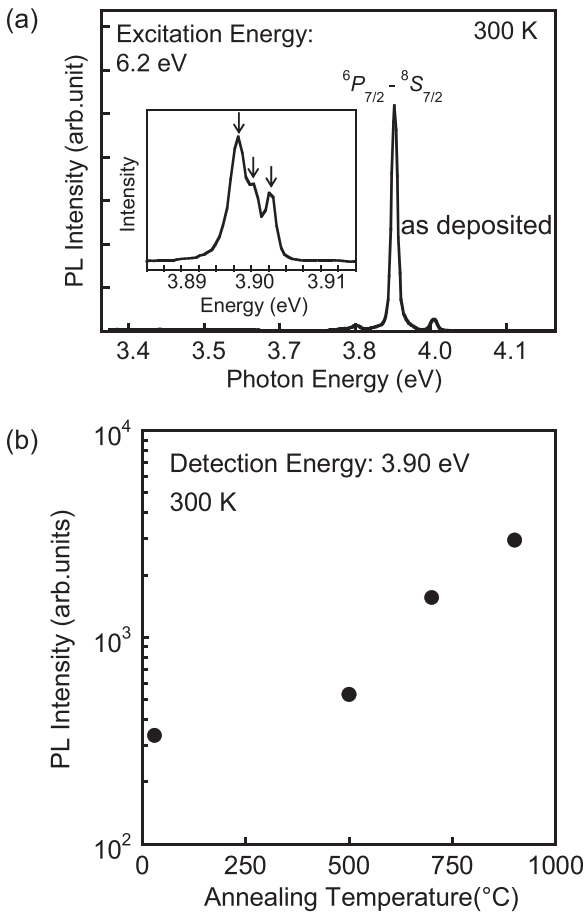

FIG. 1. (a) PL spectrum of $Al_{0.997}Gd_{0.003}N$/AlN thin films measured at 300 K. The inset shows the high-resolution PL. (b) Annealing temperature dependence of the PL-peak intensity.

the lowest excited state $^6P_{7/2}$ of Gd^{3+} in AlN splits into four levels by means of the cathodoluminescence spectroscopy and lattice-sum calculation in the C_{3v} point group symmetry; they observed (calculated) the crystal-field splitting energies of $^6P_{7/2}$ at 3.8960 (3.8953), 3.8969 (3.8958), 3.8986 (3.8992), and 3.9012 (3.9015) eV.[13] Conversely, the PL we observed exhibits only three peaks as indicated by arrows in the inset of Fig. 1(a). This discrepancy is caused by the spectral resolution of 1.5 meV in our setup, which is poorer than the crystal-field splitting energies between the lowest two Stark levels of $^6P_{7/2}$. The peak energies and the relative intensities of these fine structures were almost independent of the annealing temperature. This indicates that the thermal annealing does not significantly change the local atomic configuration of Gd^{3+}.

Figure 1(b) shows the PL-peak intensity as a function of the thermal annealing temperature. These data are taken at 300 K. Thermal annealing dramatically enhances the PL intensity, which increases approximately ten times by thermal annealing at 900 °C. Since the oscillator strength of the Gd^{3+} center, which should be sensitive to a change in the local configuration, is independent of annealing, the observed PL intensity enhancement is considered to arise from improving the efficiency of energy transfer from AlN to Gd^{3+}.

The optical absorption spectrum was measured at 300 K for the as-deposited $Al_{0.997}Gd_{0.003}N$/AlN thin film. Figure 2(a) shows the spectrum. The absorbance gradually starts increasing the magnitude above ~5.0 eV. The band-gap energy was estimated using a well-known relation between absorption signal given by $(\alpha E)^2$ and the photon energy E. The plot of the absorption signal $(\alpha E)^2$ for a semiconductor with a direct-band gap indicates a linear dependence for E in which the intercept energy for the slope of $(\alpha E)^2$ corresponds to the direct band gap. The estimated band-gap energy was 5.90 eV. This is smaller than the value of 6.03 eV for bulk AlN.[28,29] The optical absorption profile was almost independent of the post-thermal annealing. The red-shift of the band gap is caused by several reasons. The band tail structure was obvious near the band gap, however, which can be distinguished from the linear dependence of $(\alpha E)^2$ representing the bulk absorption edge. On the other hand, we have to pay attention to the optical bowing. According to our earlier work,[30] the band edge red-shifts with the increase in GdN-mole fraction. However, due to the small GdN-mole fraction x of 0.003, the red-shift caused by the alloy effect is negligible. Thus, we considered that the red-shift arises from the thermal expansion mismatch between the $Al_{0.997}Gd_{0.003}N$/AlN thin film and the fused silica substrate. In order to confirm the strain effect, we have grown the same film on a c-plane sapphire substrate. The deposited film was epitaxially grown on the sapphire substrate. The absorption profile obtained from the film on the sapphire substrate exhibits almost the same lineshape except for the edge energy. This indicates that the crystal quality of the film on a fused silica substrate is comparable with the epitaxial film. Besides, the band-edge energy was approximately 6.0 eV which is close to the bulk value. The important difference causing such band-gap shift is the thermal expansion coefficient. The thermal expansion coefficient of AlN, fused silica, and sapphire are 4.4×10^{-6}, $\sim 6 \times 10^{-7}$, and 7.0×10^{-6} K^{-1}, respectively.[21] The thermal expansion coefficient of AlN is approximately one order larger than that of fused silica. Conversely, when AlN is grown on a c-plane sapphire substrate with almost the same thermal expansion coefficient, the film is epitaxially grown and its band gap becomes close to the bulk value. From these results, we concluded that the 130 meV red-shift with respect to the band-gap energy from the literature is dominantly caused by the biaxial tensile strain in the film at room temperature.

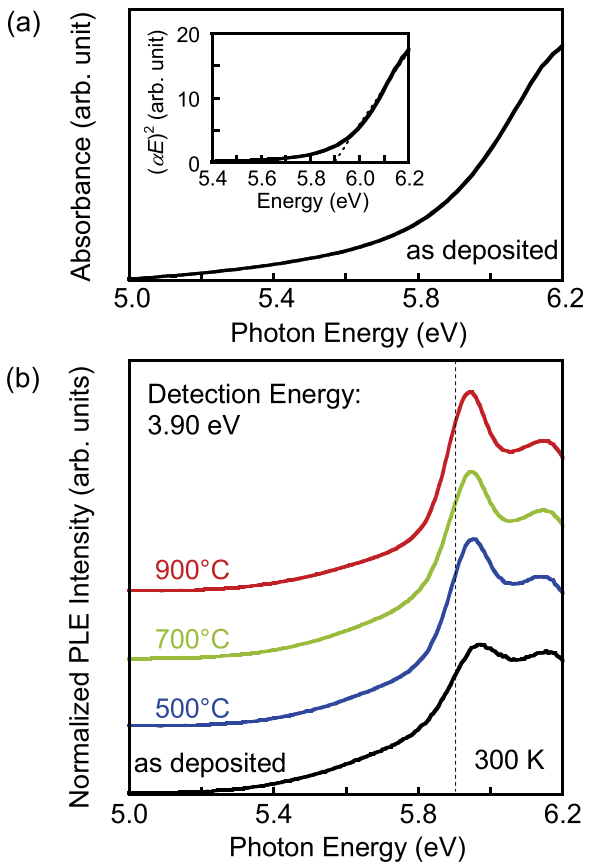

FIG. 2. (a) Optical absorption spectra of an as-deposited $Al_{0.997}Gd_{0.003}N$/AlN thin film measured at 300 K. (b) PLE spectra for $Al_{0.997}Gd_{0.003}N$/AlN thin films annealed at different temperatures. PLE spectra were measured at 300 K, and the PL-detection energy was 3.9 eV.

We measured the PLE spectrum detected at the PL peak of 3.9 eV (318 nm). The PLE spectra measured for the $Al_{0.997}Gd_{0.003}N$/AlN thin films at 300 K are shown in Fig. 2(b). In this display, the PLE intensity was normalized at 6.2 eV. In addition to the strong increase of PL intensity when excited above the fundamental absorption edge, we observed an intense absorption peak at 5.95 eV.[21] Such a peak structure never appears in the optical absorption spectrum shown in Fig. 2(a). The PLE-peak energy is close to the excited $4f$ energy levels of ^6G_J in Gd^{3+}, whereas PL enhancement was not confirmed at the other excited levels such as ^6D_J and ^6I_J of Gd^{3+}. Here, it is noted that the PLE peak in Fig. 2(b) seems to shift with annealing temperature. However, this is caused by superimpose of the resonant peak on the bulk absorption profile; the peak position of the superimposed curve shifts with decreasing the resonant-peak intensity. The observed PLE peak is attributed to an efficient

energy transfer from the band edge of AlN to the higher excited ^6G_J states of Gd^{3+}. Optically created excitons (dipoles) in AlN interact with the electronic states of Gd^{3+}, and energy collected by the host AlN is efficiently transferred to Gd^{3+} ions, which causes an increase in the excitation cross-section for Gd^{3+}.[21]

The PLE-peak energy of 5.95 eV was larger than the bandgap of 5.90 eV. The energy difference between them is approximately 50 meV, which can be attributed to the longitudinal-optical (LO) phonon energy. The A_1-symmetry LO phonon energy of bulk AlN is approximately 81 meV.[31] According to a simple linear-chain vibration model comprising two bodies, the optical-phonon energy is proportional to the square of the inverse of the reduced mass. From this relation, the optical-phonon energy of the local vibration of the Gd-N bond is estimated to be approximately 65 meV, which is moderately close to the measured energy difference. Excitons created in AlN are inelastically scattered in k space, where the exciton-phonon interaction in AlN is strong[32] because of the small dielectric constant of AlN and the resultant strong Coulomb interaction. Thus, efficient energy transfer into Gd^{3+} centers can take place. The PLE-peak intensity in Fig. 2(b) reflecting the exciton-phonon interaction increases with the annealing temperature, which causes the slight peak shift as mentioned above.

IV. THERMAL ANNEALING EFFECTS ON ENERGY TRANSFER FROM AlN TO Gd^{3+} CENTERS

We studied the temperature dependence of the PL decay. The time-resolved PL was measured at 13 and 300 K. Figure 3(a) shows typical PL-decay curves of the $Al_{0.997}Gd_{0.003}N$/AlN thin films measured at 13 K. Here, the PL intensity was normalized at 0 s. The decay curve exhibits a single exponential profile. The evaluated decay times as a function of the thermal annealing temperature are summarized in Fig. 3(b). The decay time becomes long by increasing the annealing temperature. Furthermore, the decay at 300 K becomes slow as compared with that at 13 K. The PL-decay time depends on the excited energy levels of Gd^{3+} playing as the energy acceptor. The $^6G_{11/2,\ 9/2,\ 5/2}$ states located above the $^6G_{7/2}$ state of Gd^{3+} rather interact with the conduction band of AlN. This energy transfer is dominant at 13 K. Conversely, when the temperature raised at 300 K, the AlN band edge becomes low and starts interacting with the $^6G_{7/2}$ state located below the $^6G_{11/2,\ 9/2,\ 5/2}$ states. According to our recent study reported in Ref. 21, the luminescence caused by the energy transfer into the $^6G_{11/2,\ 9/2,\ 5/2}$ states shows a relatively fast decay. The interaction also causes energy back-transfer from the Gd^{3+} centers to the host crystal. Thus, the stronger interaction gives rise to the faster PL decay.

As we mentioned above, because the local configuration of Gd^{3+} was insensitive to the thermal annealing, the oscillator strength of the Gd^{3+} center is considered to be independent of thermal annealing. A possible scenario explaining the increase in the PL intensity is that the efficiency of energy transfer from AlN to Gd^{3+} was improved by thermal annealing. The long PL-decay time observed in the annealed film supports this scenario, if the thermal annealing restrains energy dissipation of excited excitons (carriers) in AlN.

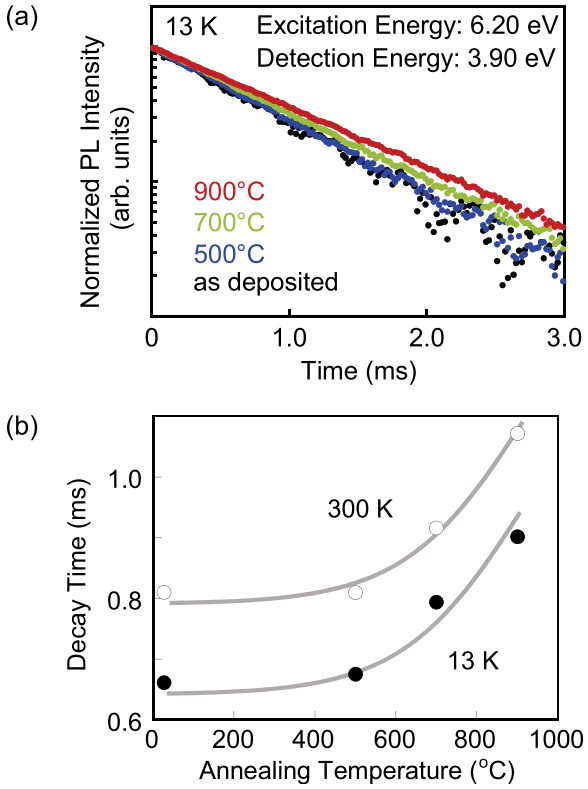

FIG. 3. Typical PL decay curves of $Al_{0.997}Gd_{0.003}N$/AlN thin films annealed at different temperatures. The measurement was carried out at 300 K. The excitation energy was 6.2 eV, and the detection energy was 3.9 eV. (b) Annealing temperature dependence of the PL decay time measured at 13 and 300 K.

Here, we need to consider effects of oxidation of the AlN film by thermal annealing on the change in the PL intensity. Oxygen is a well-known impurity in AlN crystals. The oxygen content of bulk AlN was reported to be in the order of $10^{19}\,cm^{-3}$. As we described, the oxygen content of our as-deposited film was approximately $1.0 \times 10^{19}\,cm^{-3}$. Thermal annealing carried out in our experiments caused further oxidation even under the continuous flow of highly purified N_2. The SIMS analysis gives evidence of an increase in the oxygen content in the annealed film. The average oxygen content in the annealed film was in the order of $10^{20}\,cm^{-3}$. To confirm influence of oxygen impurities on the PL, we measured oxygen-related mid-gap PL.[33] Figure 4 shows PL and PLE spectra measured at 13 K for the as-deposited and 900 °C-annealed films. The oxygen-related PL becomes weak with an increase in the measurement temperature and disappeared at 300 K. The oxygen-related PL signals are, generally, attributed to donor (D)–acceptor (A) pairs (D: oxygen in the N site and A: Al vacancy).[27] The PL-peak intensity observed at the 5.34 eV excitation was almost independent of thermal annealing. However, by comparing the PLE spectra taken from the films before and after annealing, it is obvious that a part of the PLE structures was drastically reduced by the annealing. In particular, we note the PLE-signal reduction confirmed near the band edge of AlN. The PLE spectrum of the as-deposited film shows a gradual increase in the PL

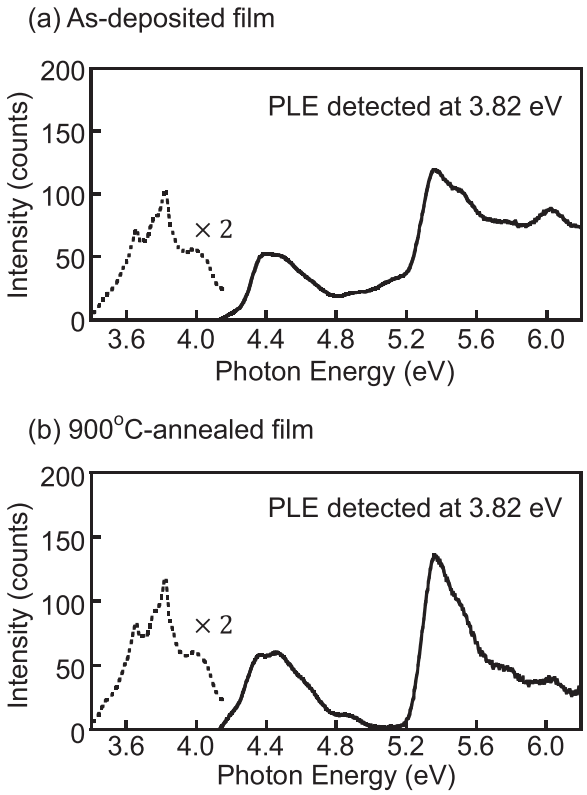

FIG. 4. Oxygen-related PL (dotted line) and PLE (solid line) spectra for (a) as-deposited and (b) 900 °C-annealed films at 13 K.

intensity with increasing the excitation photon energy, suggesting energy transfer from AlN to oxygen-related impurity centers occurs. Conversely, after thermal annealing, the PL signal caused by the energy transfer from the host crystal diminishes. This indicates that thermal annealing breaks paths of the energy transfer connecting between oxygen-related impurity centers and AlN. This peculiar puzzle can be interpreted, if we consider that excess oxygen atom occupies Al vacancies, which makes the D-A pairs vanish. The deep mid-gap D-A pair states capture carriers excited in AlN. Thus, the excess oxidation by thermal annealing reduces the density of the trap states in AlN and improves the efficiency of the energy transfer. The long PL-decay time of the 3.9 eV line observed in the annealed films is a direct evidence of the reduction of the energy dissipation in the trap centers.

V. SUMMARY

Energy transfer from AlN to doped Gd^{3+} ions as a function of post-thermal annealing temperature has been systematically investigated. Gd-doped AlN thin films were deposited on fused-silica substrates using a reactive RF magnetron sputtering technique. The intra-orbital electron transition in Gd^{3+} showed an atomically sharp luminescence at 3.9 eV (318 nm). The PLE spectrum detected at 3.9 eV shows an intense absorption peak demonstrating a resonant energy transfer from AlN to Gd^{3+} centers. We concluded that carriers excited in AlN are inelastically scattered by phonons in k space and that the efficient energy transfer into Gd^{3+} centers can take place. The energy transfer strongly depends on post-thermal annealing. Thermal annealing dramatically enhances the PL intensity, because carrier dissipation in the trap centers in AlN was reduced by thermal annealing.

[1]J. A. Parrish and K. F. Jaenicke, J. Invest. Dermatol. **76**, 359 (1981).
[2]M. Norval, L. O. Björn, and F. R. de Gruijl, Photochem. Photobiol. Sci. **9**, 11 (2010).
[3]H. Hirayama, S. Fujikawa, N. Noguchi, J. Norimatsu, T. Takano, K. Tsubaki, and N. Kamata, Phys. Status Solidi A **206**, 1176 (2009).
[4]A. Bhattacharyya, T. D. Moustakas, L. Zhou, D. J. Smith, and W. Hug, Appl. Phys. Lett. **94**, 181907 (2009).
[5]H. Hirayama, Y. Tsukada, T. Maeda, and N. Kamata, Appl. Phys. Express **3**, 031002 (2010).
[6]G. Sun, Y. J. Ding, G. Liu, G. S. Huang, H. Zhao, N. Tansu, and J. B. Khurgin, Appl. Phys. Lett. **97**, 021904 (2010).
[7]M. A. Khan, M. Shatalov, H. P. Maruska, H. M. Wang, and E. Kuokstis, Jpn. J. Appl. Phys. **44**, 7191 (2005).
[8]X. Wu, U. Hömmerich, J. D. Mackenzie, C. R. Abernathy, S. J. Pearton, R. N. Schwartz, R. G. Wilson, and J. M. Zavada, Appl. Phys. Lett. **70**, 2126 (1997).
[9]D. S. Lee and A. J. Steckl, Appl. Phys. Lett. **81**, 2331 (2002).
[10]J. H. Park and A. J. Steckl, Appl. Phys. Lett. **85**, 4588 (2004).
[11]R. Wang and A. J. Steckl, J. Cryst. Growth **312**, 680 (2010).
[12]A. Wakahara, H. Sekiguchi, H. Okada, and Y. Takagi, J. Lumin. **132**, 3113 (2012).
[13]J. B. Gruber, U. Vetter, H. Hofsäss, B. Zandi, and M. F. Reid, Phys. Rev. B **69**, 195202 (2004).
[14]U. Vetter, J. Zenneck, and H. Hofsäss, Appl. Phys. Lett. **83**, 2145 (2003).
[15]J. M. Zavada, N. Nepal, J. Y. Lin, H. X. Jiang, E. Brown, U. Hömmerich, J. Hite, G. T. Thaler, C. R. Abernathy, S. J. Pearton, and R. Gwilliam, Appl. Phys. Lett. **89**, 152107 (2006).
[16]M. Maqbool, I. Ahmad, H. H. Richardson, and M. E. Kordesch, Appl. Phys. Lett. **91**, 193511 (2007).
[17]T. Toyama, J. Ota, D. Adachi, Y. Niioka, D.-H. Lee, and H. Okamoto, J. Appl. Phys. **105**, 084512 (2009).
[18]K. Fukui, S. Sawai, T. Ito, S. Emura, T. Araki, and A. Suzuki, Phys. Status Solidi C **7**, 1878 (2010).
[19]S. Kitayama, H. Yoshitomi, S. Iwahashi, J. Nakamura, T. Kita, Y. Chigi, T. Nishimoto, H. Tanaka, M. Kobayashi, T. Ishihara, and H. Izumi, J. Appl. Phys. **110**, 093108 (2011).
[20]K. Ichii, S. Kitayama, S. Iwahashi, J. Nakamura, V. S. Reddithota, T. Kita, Y. Chigi, T. Nishimoto, H. Tanaka, M. Kobayashi, T. Ishihara, and H. Izumi, J. Phys.: Conf. Ser. **417**, 012049 (2013).
[21]Y. Ishizu, K. Tsuji, Y. Harada, T. Kita, Y. Chigi, T. Nishimoto, H. Tanaka, M. Kobayashi, T. Ishihara, and H. Izumi, J. Appl. Phys. **115**, 173508 (2014).
[22]J. M. Zavada, S. X. Jin, N. Nepal, J. Y. Lin, H. X. Jiang, P. Chow, and B. Hertog, Appl. Phys. Lett. **84**, 1061 (2004).
[23]A. Nishikawa, T. Kawasaki, N. Furukawa, Y. Terai, and Y. Fujiwara, Appl. Phys. Express **2**, 071004 (2009).
[24]T. F. Kent, S. D. Carnevale, and R. C. Myers, Appl. Phys. Lett. **102**, 201114 (2013).
[25]T. Kita, S. Kitayama, M. Kawamura, O. Wada, Y. Chigi, Y. Kasai, T. Nishimoto, H. Tanaka, and M. Kobayashi, Appl. Phys. Lett. **93**, 211901 (2008).
[26]S. Iwahashi, N. Kishi, S. Kitayama, T. Kita, Y. Chigi, T. Nishimoto, H. Tanaka, M. Kobayashi, T. Ishihara, and H. Izumi, J. Appl. Phys. **111**, 083526 (2012).
[27]A. Uedono, S. Ishibashi, S. Keller, C. Moe, P. Cantu, T. M. Katona, D. S. Kamber, Y. Wu, E. Letts, S. A. Newman, S. Nakamura, J. S. Speck, U. K. Mishra, S. P. DenBaars, T. Onuma, and S. F. Chichibu, J. Appl. Phys. **105**, 054501 (2009).
[28]Q. Guo, M. Nishio, H. Ogawa, and A. Yoshida, Phys. Rev. B **64**, 113105 (2001).
[29]Q. Guo and A. Yoshida, Jpn. J. Appl. Phys. Part 1 **33**, 2453 (1994).
[30]S. Kitayama, T. Kita, M. Kawamura, O. Wada, Y. Chigi, Y. Kasai, T. Nishimoto, H. Tanaka, and M. Kobayashi, IOP Conf. Ser.: Mater. Sci. Eng. **1**, 012001 (2009).
[31]Group IV Elements, IV-IV and III-V Compounds. Part b—Electronic, Transport, Optical and Other Properties, in *Landolt-Börnstein - Group III Condensed Matter*, edited by O. Madelung, U. Rössler, and M. Schulz (Springer, 2002), Vol. 41A1b, pp. 1–10.
[32]A. Sedhain, J. Li, J. Y. Lin, and H. X. Jiang, Appl. Phys. Lett. **95**, 061106 (2009).
[33]X. Tang, F. Hossain, K. Wongchotigul, and M. G. Spencer, Appl. Phys. Lett. **72**, 1501 (1998).